Compact Microstrip IF Lossy Filter With Ultra-Wide Stopband

Jia Ni, Jiasheng Hong, *Fellow, IEEE*, and Petronilo Martin Iglesias

***Abstract*— A novel compact six-pole intermediate frequency lossy filter based on double-layer microstrip coupled microstrip resonators is proposed in this paper. A detailed theoretical analysis for the performance operation mechanism is illustrated. Significant advantages of the proposed structure over existing lossy filters include its low passband insertion loss variation, compact footprint, and ultra-wide stopband bandwidth. Excellent experimental results are provided to confirm these improvements, by using LCP bonded PCB multilayer technology. In general, the fabricated prototype filter operates at 0.97 GHz, with 0.19-dB insertion loss variation in the passband. In addition, it obtains a sharp selectivity with a pair of transmission zeros, as well as the 10th harmonic suppression with better than the 32-dB rejection level. Good agreement between the measured and simulated results can be observed finally.**

***Index Terms*— Compact footprint, lossy technique, microstrip intermediate frequency (IF) filter, ultra-wide stopband.**

I. Introduction

AN INTERMEDIATE frequency (IF) filter is often used to block potentially interfering spectral inputs from creating distortion downstream in the receiver where amplification is provided. Often, stringent filtering requirements exist for planar and drop-in receiver filters at IF frequencies, demanding for compact footprint, a flat transmission in the passband, a high selectivity, a broad spurious-free frequency band, and low cost and weight. However, the absolute passband insertion loss and power-handling performance become less critical, since it can be easily compensated by means of that the power amplification stages located before and/or after the filter.

In the open literature, there have been many publications on the bandpass filter with a compact size and wide stopband, such as [1]–[3]. However, none of them put attention to the in-band performance for a flat passband. Recently, a new class of microwave low-cost filter, known as the planar lossy filter [4]–[11], have been attracted a lot of attention. These filters are mostly designed by using microstrip hairpin resonator [4]–[7], microstrip dual-/triple-mode resonators [8]–[10], and substrate integrated waveguide resonator [11], along with applying the technique of nonuniform-Q distribution or resistive cross couplings (RCCs) to improve the selectivity and passband flatness at the cost of increased absolute insertion loss. However, it can be found that most of these lossy filters suffered from a large footprint and/or poor stopband performance. For example, Basti *et al.* [6] presented several designs of six-pole microstrip lossy filters with promising passband flatness, by using inline and transversal networks, whereas all of these designs occupied a quite large circuit size, varying from 290 to 610 mm^2 at $f_0 = 3.8$ GHz. In addition, it is obvious to see these presented filters obtained limited stopband performance, particularly for the transversal filters. The measured 20-dB rejection bandwidths of the proposed inline and transversal filters were up to 2.5 and 0.5 GHz individually. Indeed, these drawbacks, i.e., large circuit size and poor stopband, can also be found in another design of six-pole transversal filter presented in [4]. For size reduction, dual-mode [8], [9] and triple-mode [10] microstrip resonators are employed to design the third- and/fourth-order nonuniform-Q filters. However, these presented designs also have a limited rejection frequency range of the upper stopband, resulting from their modified transversal topologies.

In this paper, a novel and compact six-pole IF lossy filter by utilizing double-layer coupled microstrip resonator structures is designed, fabricated, and tested, considering the specifications detailed in Table I. Although the characteristics of the double-layer coupled resonator structure for size reduction have been fully described in [12], several other novel measures are further taken in this paper to achieve the desired IF filtering specifications. Generally speaking, in order to flatten the passband, RCCs are introduced between the source/load and middle resonators, associated with a pair of transmission zeros created to increase the selectivity. In addition, the approach to embed tiny low-pass units with the feed structure in an integrated filter design is employed to accomplish an ultra-wide stopband with a deep rejection level. To the author's knowledge, this is the first time to discuss RCCs in compact double-layer coupled resonator filter designs, instead of hairpin resonators. Also, such a high-order microstrip lossy filter with compact size, sharp selectivity, and ultra-wide stopband with deep rejection level has not previously been reported.

II. Initial Design: Double-Layer Coupled Resonator Filter With Transmission Zeros

As can be seen in Table I, one of the challenging specifications in this paper is to design a bandpass filter centered

Manuscript received September 24, 2017; revised January 25, 2018 and April 29, 2018; accepted July 7, 2018. This work was supported by European Space Agency under Contract 4000110895/14/NL/GLC. *(Corresponding author: Jia Ni.)*

J. Ni and J. Hong are with the Institute of Sensors Signals and Systems, Heriot-Watt University, Edinburgh EH14 4AS, U.K. (e-mail: j.ni@hw.ac.uk; j.hong@hw.ac.uk).

P. M. Iglesias is with European Space Agency, 2200 AG Noordwijk, The Netherlands (e-mail: petronilo.martin.iglesias@esa.int).

Color versions of one or more of the figures in this paper are available online at http://ieeexplore.ieee.org.

Digital Object Identifier 10.1109/TMTT.2018.2858781

TABLE I
SPECIFICATION OF THIS PAPER

PARAMETERS	SPEC.	Unit
Center frequency (f_0)	1000	MHz
Channel Bandwidth	250	MHz
Insertion loss (IL) at f_0	TBA	dB
IL variation versus Frequency		
$f_0 \pm 70$ MHz	<0.25	dB
$f_0 \pm 100$ MHz	<0.6	dB
$f_0 \pm 120$ MHz	<1.5	dB
Narrowband isolation		
$f_0 \pm 160$ MHz	>20	dB
$f_0 \pm 400$ MHz	>30	dB
Out of-band rejection		
$f_0 + 400$ MHz to$10f_0$	>30	dB
Footprint	20×20	mm^2

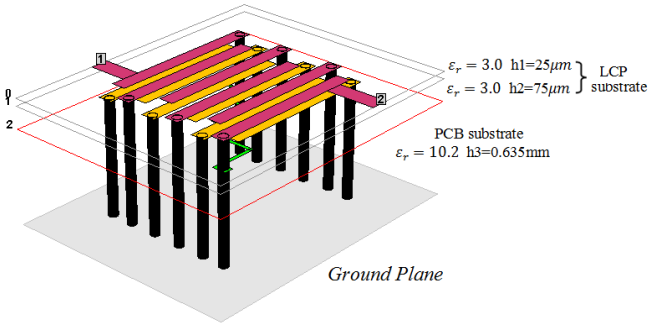

(a)

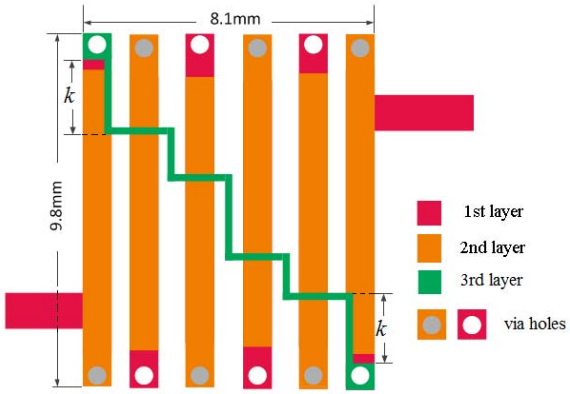

(b)

Fig. 1. (a) 3-D view of initial design with detailed information of LCP boned PCB multilayer technology. (b) Layout of the third layer of initial design.

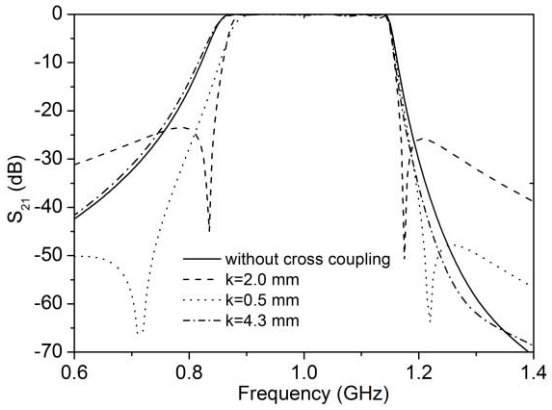

Fig. 2. Controlling of transmission zeros versus different overlap lengths k of crossing line.

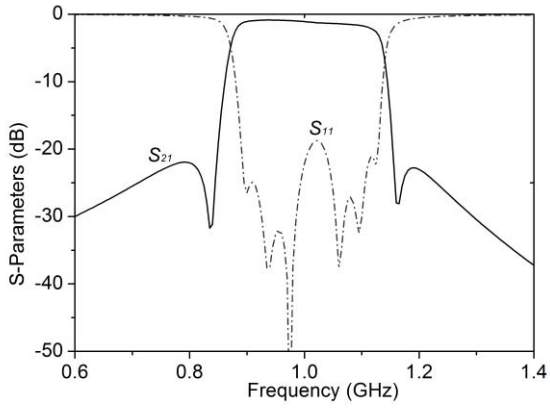

(a)

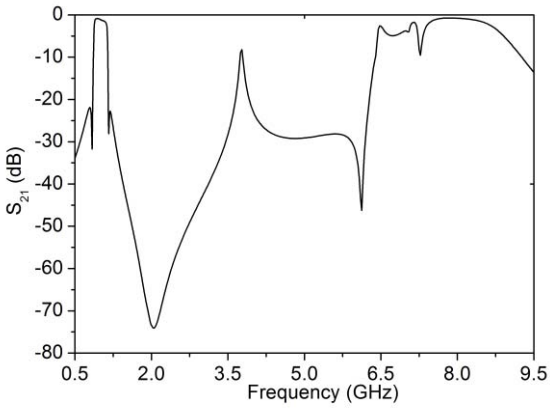

(b)

Fig. 3. Simulated frequency response of initial design. (a) Passband performance. (b) Stopband performance.

at 1 GHz (NB free-space wavelength = 300 mm) within a compact circuit size of 20 mm × 20 mm. To this end, the double-layer coupled resonator proposed in [12] is employed for our initial design, since such a resonator structure has good features of size reduction and broad stopband. The detailed theoretical descriptions of a double-layer coupled resonator can be found in [12] and not repeated here. However, different from the work presented in [12], the resonator is realized in terms of microstrip by using a low-cost LCP bonded multilayer PCB technology. In addition, in order to increase selectivity, a pair of transmission zeros is created and discussed in our proposed filtering structure that is shown in Fig. 1. As can be found, a crossing line located in the third layer is utilized to connect between the first and sixth resonators. Inspecting the frequency responses shown in Fig. 2, it is notable that with the help of such a crossing line, a transmission zero can be introduced at each side of the passband, leading to an enhanced selectivity. The TZs can be controlled by varying the dimension (k) of the stub. As can be seen, with a proper k

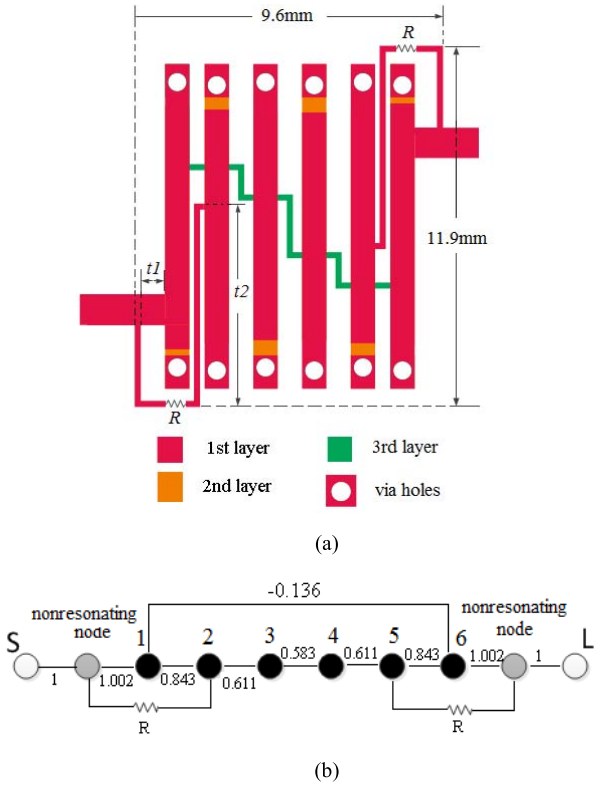

Fig. 4. (a) Layout of IF filter I with improved passband flatness by using RCCs. (b) Associated coupling diagram with normalized coupling coefficient for initial design.

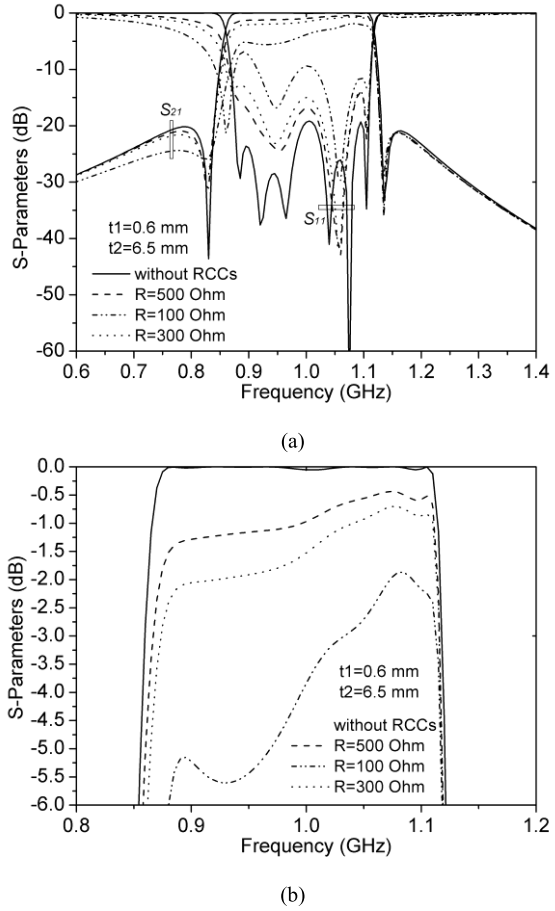

Fig. 5. Effect of resistors that applied in RCCs on (a) filtering shape and (b) insertion loss variation in the passband.

of 0.5 mm, a pair of symmetrical TZs is obtained. However, it is interesting to see, when k is increased to 4.3 mm, the pair of transmission zeros disappear, which would imply that the crossing line, in this case, does not provide a proper cross coupling for TZ creation [13].

Fig. 3 shows the frequency responses of the initial design are plotted, after considering all the dissipation losses. Obviously, the lossy case suffers from more insertion losses or more rounded-off band edges at the upper part of the passband, exhibiting around 1-dB difference. However, excluding passband flatness and stopband bandwidth constraints, such initial design is promising, particularly in terms of compact footprint and selectivity. In Section III, the objective of this paper is to improve the flatness by designing lossy filters as well as improving the stopband performance.

III. Design of IF Filter With Improved Passband Flatness

It is well known that the principle of most published lossy filters is to design a prototype filter that has peak transmission response near the passband edges by deliberately adding or distributing more losses in the midband, to compensate for rounded-off passband edges. However, herein, in order to flatten the passband, introducing additional losses at the lower part of passband instead of midband is required, since the proposed initial design obtained maximum power transmission in the lower side of passband [see Fig. 3(a)]. In this regard, two identical RCCs are introduced to the initial design, as the structure (namely, "IF filter I") demonstrated in Fig. 4(a), which are mostly used to absorb more power at the lower side of passband rather than the upper one. The associated coupling diagram is also shown in Fig. 4(b), where the normalized coupling coefficients are provided to produce initial physical dimensions. In terms of practical realizations of RCCs, it can be noted that the resistors directly connect the second/fifth resonator to nonresonating nodes, with capacitive coupling nature. In this case, we do not need any electrical length of 90° or 360° transmission lines for scaling, like the ones in [6] and [14], leading to a reduced circuit size. Theoretically, such coupling is mainly controlled by the tapped positions (parameters $t1$ and $t2$) as well as the value of the resistor. For our investigation, first Fig. 5 shows a set of frequency responses by only varying the values of the resistor, i.e., R, compared with the initial lossless design without RCCs. Generally, as can be seen in Fig. 5(a), by virtue of RCCs, there are more insertion losses produced at the lower part of passband rather than the upper one. In the meantime, the return loss is degraded more at the lower side of the passband. In detail, as shown in Fig. 5(b), when the resistance R is changing from 500 to 100 Ω, the difference of insertion loss

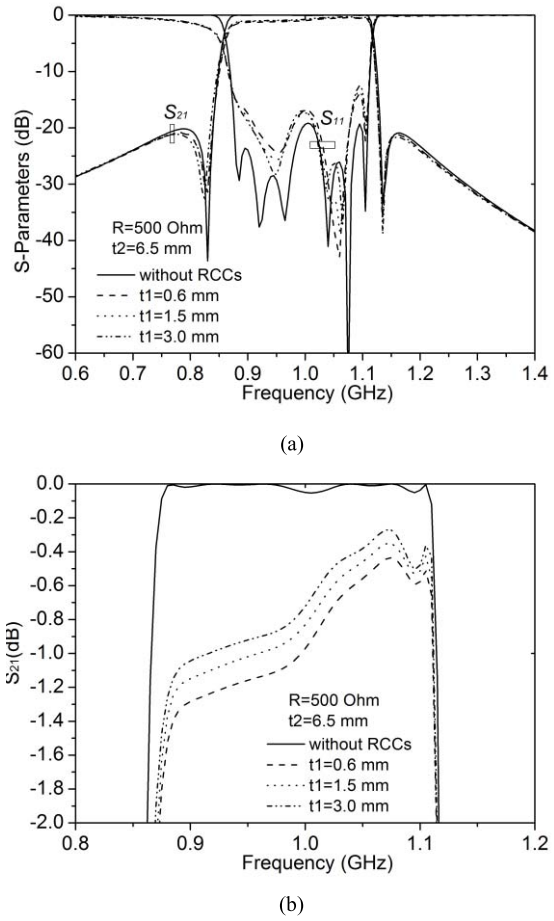

Fig. 6. Effect of tapped position "$t1$" of RCCs on (a) filtering shape and (b) insertion loss variation in the passband.

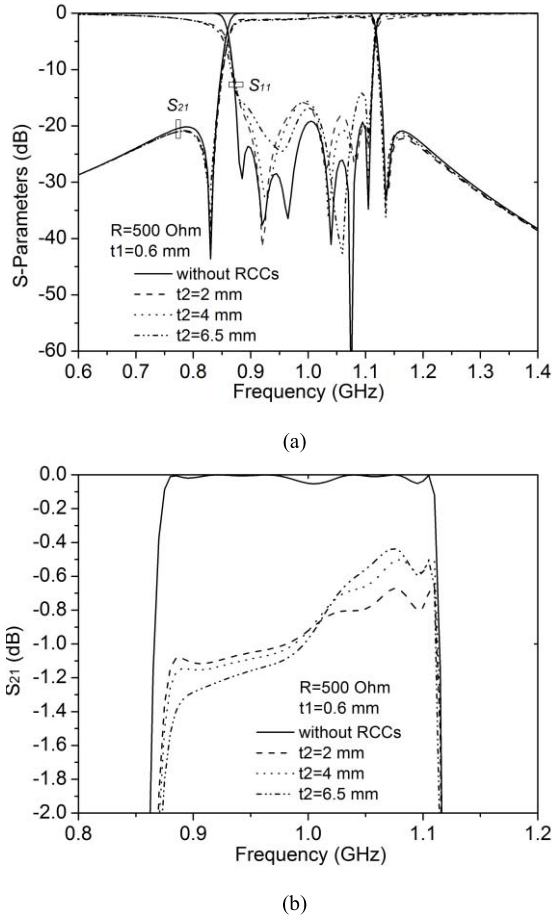

Fig. 7. Effect of tapped position "$t2$" of RCCs on (a) Filtering shape. (b) Insertion loss variation in the passband.

levels between lower and upper band edges become more prominent, with the variation of 1.9 and 3.2 dB, respectively.

Figs. 6 and 7 show the frequency responses achieved by individual tuning the tapped positions $t1$ and $t2$, in comparison to the initial state as well. In contrast to the above case of adjusting R, varying the tapped positions has much less degradation on the return loss as well as the rejection level on TZs. In an aspect of passband insertion loss, both cases obtain more rounded-off lower passband edge. In particular, for the case illustrated in Fig. 6(b), it is interesting to see by changing parameter $t1$ from 3.0 to 0.6 mm, the insertion loss is almost increased proportionally, remaining the same loss variation of 0.8 dB along the passband. While noting the other case shown in Fig. 7(b), the larger the $t2$, the further is the tapped line to the grounding of the resonator, which results in more insertion losses at the lower part of the passband, but less insertion loss at the upper side, with larger insertion loss variation produced.

Based on the earlier discussion, the IF filter I shown in Fig. 4(a) is optimized using Sonnet, where the parameters are set to be $t1 = 0.6$ mm, $t2 = 6.5$ mm, and $R = 500\ \Omega$. The associated frequency response is demonstrated in Fig. 8, which is compared to the initial response at the same time. It is promising to see a remarkable improvement in passband flatness for the IF filter I, as shown in Fig. 8(a), with 0.11-dB insertion loss variation within the frequency range of $f_{\mathrm{IF}} \pm 100$ MHz. The absolute insertion loss is 2.1 dB. In addition, one can observe that the return loss and the selectivity for IF filter I are hardly degraded after adding RCCs. Regarding the stopband performance, as shown in Fig. 8(b), it is notable that RCCs do not bring any significant improvement on harmonic suppression.

Indeed, the above-desired passband flatness can be achieved by only using one path of RCC. However, obviously, two RCCs could compensate each other with more flexibility during the fabrication, as well as could provide a symmetric physical layout.

IV. Design of IF Filter With Extended Stopband Bandwidth

Observing the frequency response of IF filter I shown in Fig. 8, although the second harmonic is suppressed, the stopband bandwidth is still far away from the stringent specification given in Table I. In order to obtain a broader stopband bandwidth, probably the most straightforward method is to employ additional low-pass structures to clean up the harmonics. As a rule of thumb, it is better to purposely design different low-pass units with different parameters to make

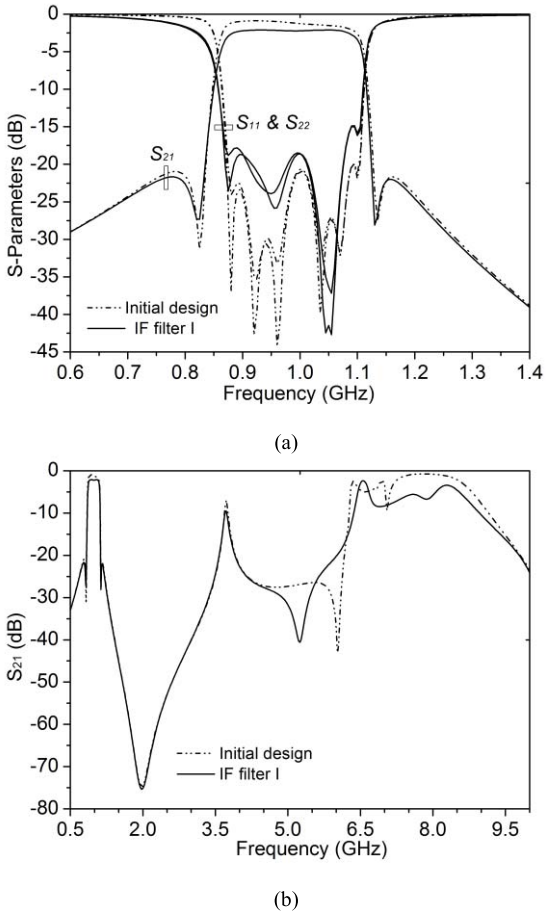

Fig. 8. Simulated frequency responses of IF filter I with improved passband flatness. (a) Passband performance. (b) Stopband performance.

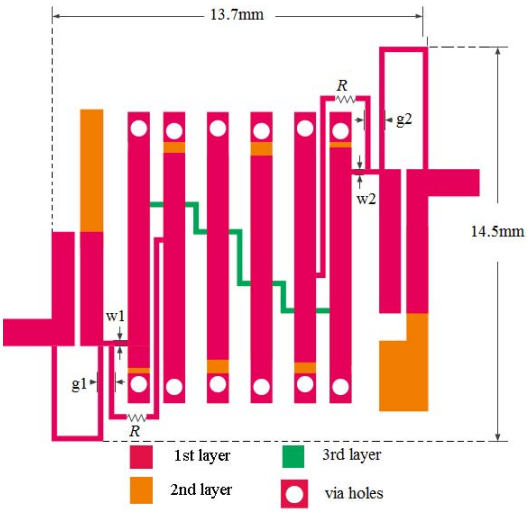

Fig. 9. Layout of IF filter II with expanded stopband bandwidth.

zeros be allocated at harmonics for suppression. Operating in this manner, Fig. 9 proposes an improved six-pole IF filter based on the design of IF filter I, namely, "IF Filter II." As can be seen, two compact multilayer low-pass filtering units with different cutoff frequencies integrate toward the

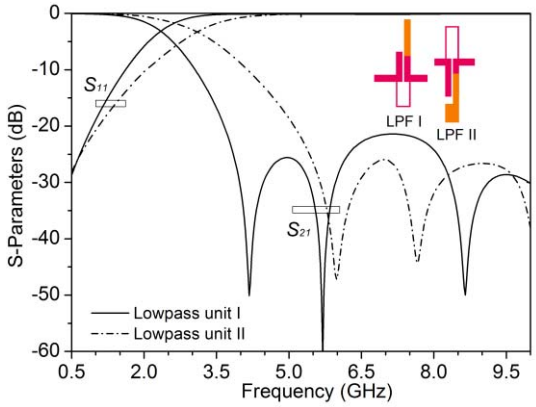

Fig. 10. Simulated frequency responses of two different low-pass filtering units for broadening the stopband bandwidth.

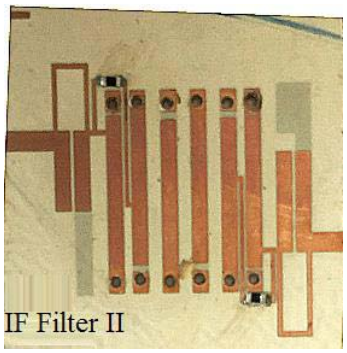

Fig. 11. Photograph of the fabricated prototype filter.

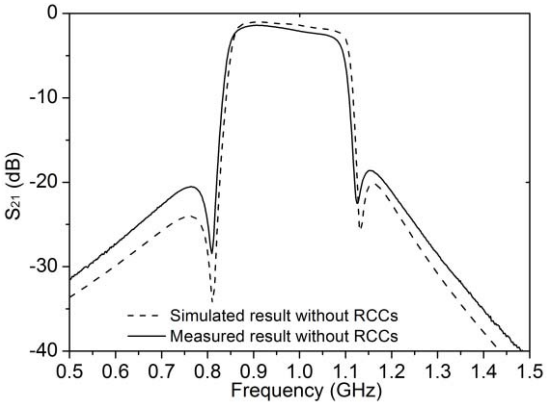

Fig. 12. Simulated and measured responses of IF filter II under the condition of R = infinite (i.e., without RCCs).

input–output feed structures of BPF section individually. Each low-pass filtering structure consists of a coupled-line hairpin unit in the first layer and one additional stub in the second layer that coupled to the first layer. Herein, the main function of such additional stub is to produce extra transmission zeros in the stopband with improved performance, while the cutoff frequency is mostly determined by the hairpin unit. For better demonstration, Fig. 10 shows the frequency responses of these two low-pass units. As can be seen, they both exhibit a wide stopband with three attenuation poles, leading to the rejection

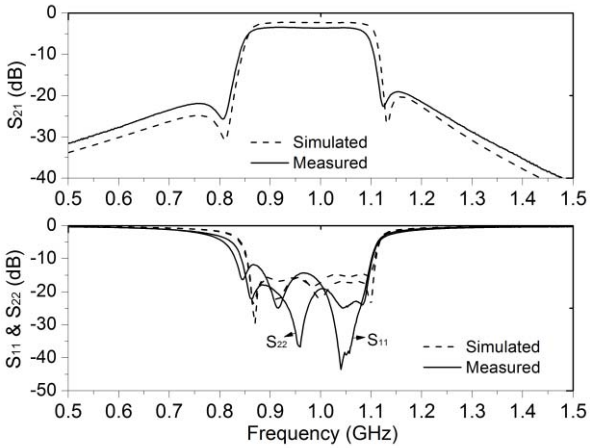

(a)

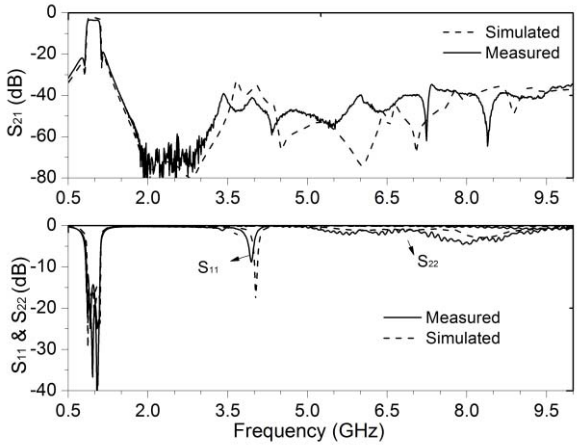

(b)

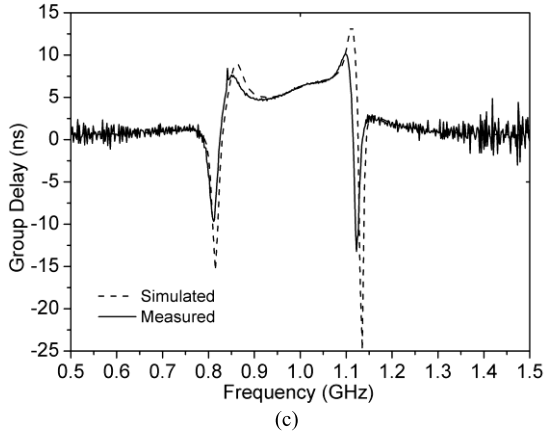

(c)

Fig. 13. Simulated and measured frequency responses of IF filter II. (a) Passband performance. (b) Stopband performance. (c) Group delay.

greater than 20 dB. Meanwhile, both low-pass units show the very low insertion loss in the desired passband with an insertion loss less than 0.12 dB and return loss better than 19 dB at 1 GHz. These characteristics offer a great possibility to expand the out-of-band rejection while almost maintaining the in-band behavior of the fundamental lossy BPF after integration. However, it should be highlighted that when designing an integrated filter, the dimensions of connecting lines (i.e., parameters $w1$, $g1$, $w2$, and $g2$ in Fig. 9) between

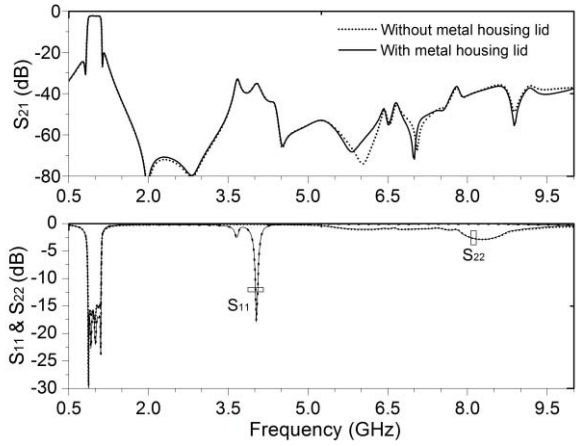

Fig. 14. Comparative responses of the proposed design with and without metal housing lid.

the low-pass and bandpass units have a remarkable effect on the stopband performance rather than passband, resulting from complex phase behaviors. In this design, the length and width of such connecting lines are optimized to have an approximate rejection level covering the whole stopband.

For experimental verification, the proposed compact IF filter II was fabricated by using the LCP bonded multilayer PCB technology that is as same as the one shown in Fig. 1(a). A detailed photograph of such fabricated sample is shown in Fig. 11, where a compact circuit size of 13.7 mm $\times$ 14.5 mm (around 0.097 $\lambda_g \times 0.103\lambda_g$, where λ_g is the guided wavelength at center frequency $f_0 = 1$ GHz). Panasonic resistors $R = 300\ \Omega$ are adopted for RCCs, instead of $R = 500\ \Omega$ used for simulation. This is because for the measured case without RCCs, a higher insertion loss is observed than the simulated one (see Fig. 12), resulting from manufacturing tolerance. The measured results along the simulated results are shown in Fig. 13. Generally, good agreement between the measured and simulated results can be observed. In detail, as can be seen in Fig. 13(a), the measured filter operated at a center frequency of 0.97 GHz with a 3-dB bandwidth 250 MHz, giving a slight frequency shifting in comparison to the desired specification demonstrated in Table I. The passband return loss is greater than 11.8 dB and the passband absolute insertion loss is 3.4 dB that is a bit larger than that of the simulated due to lower resistor employed in manufacturing. In terms of passband flatness, the measured filter obtains an insertion loss variation of 0.19, 0.3, and 1.3 dB within the frequency range of $f_0 \pm 70$, $f_0 \pm 100$, and $f_0 \pm 120$ MHz, respectively, which successfully meets the desired specifications. The shape of the measured response is equivalent to that of a conventional filter with a uniform unloaded Q of 380. In addition, the measured response achieves a pair of transmission zeros, locating at 0.8 and 1.22 GHz with the rejection level better than 19 dB. The measured narrowband isolations at frequencies $f_0 \pm 160$ and $f_0 \pm 400$ MHz are around 21 and 31 dB individually, which satisfy the design requirements as well. Regarding the stopband performance given in Fig. 13(b), the tested sample obtains a rejection level greater than 32 dB, covering the entire

TABLE II
COMPARISON BETWEEN THE PROPOSED FILTERS WITH OTHER RELATED WORKS

Ref.	Type of resonator	Order	Lossy Techniques	f_0*(GHz) /FBW	Absolute IL (dB)	Stopband width @rejection(dB)	Q_u : EQ	TZs	Size (mm × mm)
[4]	hairpin	Six	Non-uniform Q and RCCs	0.96/6.2%	7.2	1.2× f_0@40dB	250/80:750	Yes	N/A Large
[5]	hairpin	Four	RCCs	1/11.5%	3	2× f_0@30dB	200:1000	No	N/A Large
[6]	hairpin	Six	RCCs	3.8/21%	3.4/4.2	3.5× f_0@20dB	95:300	No	300mm^2
			nonuniform Q		2.5	Very poor	95/57/35:240	No	480mm^2
[7]	hairpin	Six	RCCs	1.88/8%	5.4	2.1× f_0@20dB	150:600	Yes	50× 30 ($0.8\lambda_g \times 0.48\lambda_g$)
[8]	dual-mode and hairpin	Three	Nonuniform Q	2.48/10%	1.5	2.6× f_0@12dB	280/84:540	Yes	32.4× 29.8 ($0.42\lambda_g \times 0.39\lambda_g$)
[9]	dual-mode	Four	Nonuniform Q	2.01/5.4%	6.7	N/A	180/48:970	Yes	23.06× 24.7 ($0.26\lambda_g \times 0.27\lambda_g$)
This work	**Double-layer coupled resonator (<<$1/4\lambda$)**	Six	**RCCs**	**1.0/25%**	**2.2 (simulated)**	**3.5×f_0@20dB (IF Filter I)**	**120:450**	**Yes**	**9.6× 11. 9 ($0.067\lambda_g \times 0.084\lambda_g$)**
				0.97/25.7%	**3.4 (measured)**	**10× f_0@32dB (IF Filter II)**	**120:380**	**Yes**	**13.7× 14. 5 ($0.097\lambda_g \times 0.103\lambda_g$)**
EQ: Equivalent Q-factor									

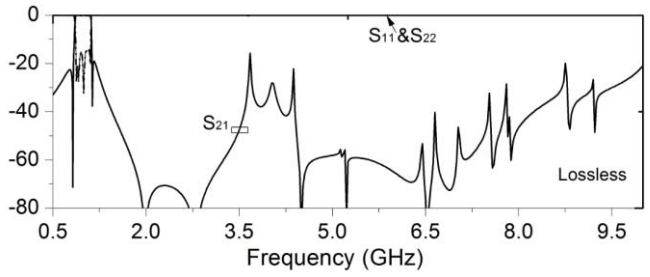

Fig. 15. Lossless response without RCCs and material losses.

stopband. Moreover, as shown in Fig. 13(c), the measured filter obtains a group delay variation of 1.8, 2.4, and 4.7 ns within the frequency range of $f_0 \pm 70$, $f_0 \pm 100$, and $f_0 \pm 120$ MHz, respectively. We have further investigated the out-of-band responses of Fig. 13(b). Fig. 14 shows a comparison of the responses with and without a metal housing lid, which are almost the same indicating that those out-of-band dips are due to the absorption of the circuit material losses as well as the loaded resistors for RCCs, but not the radiation. Furthermore, the evidence is shown in Fig. 15 where the response is assumed without the RCCs and material losses resulting in no out-of-band dips of S_{11}/S_{22}, as shown in Fig. 14. Evidently, those out-of-band dips of S_{11}/S_{22} are absorbed by the material losses including the loaded resistors in the filter. By inspecting the S_{21} responses in Figs. 14 and 15, one can see that the RCCs and material losses also enhance the out-of-band rejection. Table II summarizes performance comparison with related work in the literature. To the author's knowledge, a microstrip filter with the above-exhibited attractive performance has not previously been reported.

V. CONCLUSION

A compact six-pole IF lossy filter using double-layer coupled microstrip resonating structures has been proposed and experimentally verified, which addressed diverse aspects of filter high performance, including compact size, flat passband, sharp selectivity, and ultra-wide stopband. These promising results have been achieved using techniques based on RCC to flatten the passband, cross coupling to produce transmission zeros, and integrating low-pass units to expand stopband, together with a degree of computer optimization. To the authors' knowledge, this is the first time to discuss RCCs in double-layer coupled quarter-wavelength resonator filter designs and a microstrip lossy filter with such attractive performance will find applications in demanding subsystems including frequency converters for satellite communications.

REFERENCES

[1] K. F. Chang and K. W. Tam, "Miniaturized cross-coupled filter with second and third spurious responses suppression," *IEEE Microw. Wireless Compon. Lett.*, vol. 15, no. 2, pp. 122–124, Feb. 2005.

[2] T.-N. Kuo, W.-C. Li, C.-H. Wang, and C. H. Chen, "Wide-stopband microstrip bandpass filters using quarter-wavelength stepped-impedance resonators and bandstop embedded resonators," *IEEE Microw. Wireless. Compon. Lett.*, vol. 18, no. 6, pp. 389–391, Jun. 2008.

[3] S.-C. Lin, P.-H. Deng, Y.-S. Lin, C.-H. Wang, and C. H. Chen, "Wide-stopband microstrip bandpass filters using dissimilar quarter-wavelength stepped-impedance resonators," *IEEE Trans. Microw. Theory Techn.*, vol. 54, no. 3, pp. 1011–1018, Mar. 2006.

[4] A. C. Guyette, I. C. Hunter, and R. D. Pollard, "The design of microwave bandpass filters using resonators with nonuniform Q," *IEEE Trans. Microw. Theory Techn.*, vol. 54, no. 11, pp. 3914–3922, Nov. 2006.

[5] J. Mateu *et al.*, "Synthesis of 4th order lossy filter with uniform Q distribution," in *IEEE MTT-S Int. Microw. Symp. Dig.*, May 2010, pp. 568–571.

[6] A. Basti, S. Bila, S. Verdeyme, A. Périgaud, L. Estagerie, and H. Leblond, "Design of microstrip lossy filters for receivers in satellite transponders," *IEEE Trans. Microw. Theory Tech.*, vol. 62, no. 9, pp. 2014–2024, Sep. 2014.

[7] Z. Zhou, J. Ni, and J. Hong, "Novel lossy microstrip filter with extracted-pole technique," in *Proc. 46th Eur. Microw. Conf.*, London, U.K., Oct. 2016, pp. 120–123.

[8] J. Ni, W. Tang, J. Hong, and R. H. Geschke, "Design of microstrip lossy filter using an extended doublet topology," *IEEE Microw. Wireless Compon. Lett.*, vol. 24, no. 5, pp. 318–320, May 2014.

[9] L.-F. Qiu, L.-S. Wu, W.-Y. Yin, and J.-F. Mao, "A flat-passband microstrip filter with nonuniform-Q dual-mode resonators," *IEEE Microw. Wireless Compon. Lett.*, vol. 26, no. 3, pp. 183–185, Mar. 2016.

[10] F.-J. Chen, L.-S. Wu, L.-F. Qiu, and J.-F. Mao, "A lossy triple-mode microstrip filter with flat passband based on nonuniform Q-factors," in *Proc. Asia–Pacific Microw. Conf.*, Sendai, Japan, Nov. 2014, pp. 1139–1141.
[11] L. Szydlowski, A. Lamecki, and M. Mrozowski, "Design of microwave lossy filter based on substrate integrated waveguide (SIW)," *IEEE Microw. Wireless Compon. Lett.*, vol. 21, no. 5, pp. 249–251, May 2011.
[12] Y. Zhang, K. A. Zaki, A. J. Piloto, and J. Tallo, "Miniature broadband bandpass filters using double-layer coupled stripline resonators," *IEEE Trans. Microw. Theory Techn.*, vol. 54, no. 8, pp. 3370–3377, Aug. 2006.
[13] J.-S. Hong, *Microstrip Filters for RF/Microwave Applications*, 2nd ed. New York, NY, USA: Wiley, 2011.
[14] V. Miraftab and M. Yu, "Generalized lossy microwave filter coupling matrix synthesis and design using mixed technologies," *IEEE Trans. Microw. Theory Techn.*, vol. 56, no. 12, pp. 3016–3027, Dec. 2008.

Jia Ni received the B.Eng. degree in electrical engineering from the Nanjing University of Science and Technology, Nanjing, China, in 2008, and the Ph.D. degree from Heriot-Watt University, Edinburgh, U.K, in 2014.

Since 2014, she has been a Post-Doctoral Research Fellow with the Microwave and Antenna Engineering Group, Heriot-Watt University. Her current research interests include tunable and reconfigurable microwave filters, multilayer circuit design, microwave lossy filter, and miniature RF/microwave devices.

Jiasheng Hong (M'94–SM'05–F'12) received the D.Phil. degree in engineering science from the University of Oxford, Oxford, U.K., in 1994. His doctoral dissertation concerned electromagnetic (EM) theory and applications.

In 1994, he joined the University of Birmingham, Birmingham, U.K., where he was involved with microwave applications of high-temperature superconductors, EM modeling, and circuit optimization. In 2001, he joined the Department of Electrical, Electronic and Computer Engineering, Heriot-Watt University, Edinburgh, U.K., where he is currently a Professor leading a team on research into advanced RF/microwave device technologies. He has authored or co-authored over 200 journal and conference papers and 2 books, *Microstrip Filters for RF/Microwave Applications* (Wiley, 1st ed., 2001, 2nd ed., 2011) and *RF and Microwave Coupled-Line Circuits* (Artech House, 2nd ed., 2007). His current research interests include RF/microwave devices, such as antennas and filters, for wireless communications and radar systems, as well as novel material and device technologies including multilayer circuit technologies using package materials such as liquid crystal polymer, RF MEMS, and ferroelectric and high-temperature superconducting devices.

Petronilo Martin Iglesias was born in Caceres, Spain, in 1980. He received the Telecommunication Engineering degree from the Polytechnic University of Madrid, Madrid, Spain, in 2002 and the master's degree from The University of Leeds, Leeds, U.K., in 2012.

He has been a Microwave Engineer with the industry for more than 15 years for active (high power amplifiers for radar applications) and passive (filters, multiplexers, couplers, etc.) RF hardware design, including 2 years as a Radar System Engineer with INDRA SISTEMAS, ISDEFE S.A., and Thales Alenia Space Spain. Since 2012, he has been with research and development and project support activities related to RF passive hardware developments for the European Space Agency. His current research interests include filter synthesis theory, electromagnetic design, and high-power prediction, as well as advanced manufacturing techniques for RF passive hardware.